Two-channel passive detection of cyclostationary signals in noise with spatio-temporal structure

Stefanie Horstmann*, David Ramírez†, Peter J. Schreier*, and Aaron Pries*
*Signal and System Theory Group, University of Paderborn, Germany
Email: {stefanie.horstmann, peter.schreier, aaron.pries}@sst.upb.de
†Department of Signal Theory and Communications, Universidad Carlos III de Madrid, Spain
Gregorio Marañón Health Research Institute, Madrid, Spain
Email: david.ramirez@uc3m.es

***Abstract*—In this work, we derive a two-channel passive detector for cyclostationary (CS) signals contaminated by noise with spatio-temporal structure. This problem is motivated by a passive radar system equipped with a reference and a surveillance antenna array. Since typical illuminators of opportunity (IO) transmit CS signals, we derive a generalized likelihood ratio test (GLRT) to detect the presence of cyclostationarity at the surveillance channel (SC) given observations of both SC and reference channel under different noise assumptions. Simulation results show that exploiting cyclostationarity on the one hand and the structure of the noise on the other hand increases the performance compared to the general case of temporally colored and spatially correlated noise. Our approach also outperforms other state-of-the-art competitors.**

I. Introduction

In this paper, we consider a passive bistatic radar system that consists of an illuminator of opportunity (IO), a reference channel (RC), and a surveillance channel (SC). These systems are of special interest as they are cheap, simple and undetectable since the transmitter, which is the IO, is not part of the passive radar system itself [1]. Commonly, IOs are commercial video or audio broadcast systems or they could be space-based sources such as communication or navigation satellites [1]. In this work we consider a multiple-input multiple-output (MIMO) system in which there are a reference antenna array that receives a noisy version of the direct-path signal transmitted by the IO, and a surveillance array. This array receives the target-path signal if a target is present, or noise only, otherwise. We assume that clutter or direct-path interference, which may corrupt the signal received at the SC, is canceled by employing the techniques presented in, e.g., [2]–[4]. Furthermore, the SC and RC signals are obtained by spatial filtering [2], [5] or by employing directional antennas [6].

Commonly, this target detection problem is approached by cross-correlating SC and RC signals [1], [7], [8], which is, however, suboptimal due to noise at the RC [9]. Moreover, in the past, various generalized likelihood ratio tests (GLRT) have been derived for the case of unknown deterministic waveforms in temporally and spatially white noise [10], [11]. Also, GLRTs considering the case of stochastic waveforms in white noise with various assumptions on the spatial correlation among each array and across reference and surveillance array have been derived in [12]–[15].

These aforementioned detectors assume that the signals are temporally white. However, digital communication signals transmitted by IOs are not temporally white but cyclostationary (CS) [1], [16]. In our previous work [17], we derived the GLRT for the general case of spatially correlated and temporally colored noise. Spatial correlation refers to the correlation at the individual arrays but not across reference and surveillance arrays. When the noise has further structure, it should be exploited in the detector design. Specifically, if the antenna arrays are properly calibrated, the noise at each antenna can be considered temporally white and spatially uncorrelated. However, if the calibration fails, this assumptions may be violated. Hence, in this work, we consider noise with further structure: temporally white noise, which can be either spatially correlated or not, and temporally colored noise that is spatially uncorrelated.

We derive the GLRTs for these noise models and show that for all cases the GLRT can be factorized into the single channel GLRT [18], [19], which accounts for the presence of cyclostationarity at the SC, and a second term that accounts for the cross-cyclic correlations between observations at SC and RC. We show that exploiting cyclostationarity and, additionally, the structure of the noise increases the performance of the previously proposed detector for the general case of temporally colored and spatially correlated noise [17]. For the case that the noise structure is not known a priori, we may apply the tests proposed in [19] to specify the noise structure.

II. Problem formulation

We consider a passive bistatic radar system, which consists of a reference array and a surveillance array. The received signal at the SC is denoted by $\mathbf{u}_s[n] \in \mathbb{C}^L$ and the received signal at the RC is given by $\mathbf{u}_r[n] \in \mathbb{C}^L$, where we assumed without loss of generality that there are L antennas at both arrays. Furthermore, in our signal model we consider the true pair of time-delay and Doppler shift, which allows us to synchronize the target-path signal with the direct-path signal. Hence, the test statistic derived in this paper serves as an ambiguity score [14]. The problem considered in this paper is therefore given by the two hypotheses

$$\begin{aligned} \mathcal{H}_0 : &\begin{cases} \mathbf{u}_s[n] = \mathbf{v}_s[n], \\ \mathbf{u}_r[n] = \mathbf{H}_r[n] * \mathbf{s}[n] + \mathbf{v}_r[n], \end{cases} \\ \mathcal{H}_1 : &\begin{cases} \mathbf{u}_s[n] = \mathbf{H}_s[n] * \mathbf{s}[n] + \mathbf{v}_s[n], \\ \mathbf{u}_r[n] = \mathbf{H}_r[n] * \mathbf{s}[n] + \mathbf{v}_r[n], \end{cases} \end{aligned} \tag{1}$$

where $\mathbf{H}_s[n] \in \mathbb{C}^{L \times L_I}$ and $\mathbf{H}_r[n] \in \mathbb{C}^{L \times L_I}$ represent the frequency-selective channels between the IO and reference and surveillance arrays. The signal transmitted by the IO, which is equipped with L_I antennas, where $L_I \geq L$, is denoted by $\mathbf{s}[n] \in \mathbb{C}^{L_I}$. Moreover, $\mathbf{s}[n]$ is considered to be a discrete-time zero-mean second-order CS signal with known cycle period P. Finally, $\mathbf{v}_s[n] \in \mathbb{C}^L$ and $\mathbf{v}_r[n] \in \mathbb{C}^L$ are additive noise terms that are wide-sense stationary (WSS) and uncorrelated between RC and SC. However, within each array the noise may have further structure, which is either 1) *temporally white & spatially uncorrelated*, 2) *temporally white & spatially correlated*, or 3) *temporally colored & spatially uncorrelated*. In order to derive the GLRT we follow our work in [17] in which we have considered the case of temporally colored and spatially correlated noise.

Let us collect NP samples of each array into the vectors

$$\mathbf{y}_\clubsuit = \left[\mathbf{u}_\clubsuit^T[0], \ldots, \mathbf{u}_\clubsuit^T[NP-1]\right]^T, \tag{2}$$

for $\clubsuit \in \{s, r\}$. Before deriving the GLRT we will first investigate the structures of the (cross) covariance matrices $\mathbf{R}_{\clubsuit\heartsuit} = \mathrm{E}[\mathbf{y}_\clubsuit \mathbf{y}_\heartsuit^H] \in \mathbb{C}^{LNP \times LNP}$. Under both hypotheses the covariance matrix $\mathbf{R}_{rr}$ has the same structure. Considering that the signal $\mathbf{u}_r[n]$ is CS with cycle period P, we exploit a result from [20] that shows that the stack of P observations of a CS process is WSS, i.e. the covariance matrix $\mathbf{R}_{rr}$ is a block-Toeplitz matrix with block size LP. Following the same argument it is easy to see that under $\mathcal{H}_1$ the matrices $\mathbf{R}_{ss}^{(1)}$ and $\mathbf{R}_{sr} = \mathbf{R}_{rs}^H$ are also block-Toeplitz matrices with block size LP.[1]

Considering the null hypothesis, we should first notice that the observations from SC and RC are uncorrelated since $\mathbf{v}_s[n]$ and $\mathbf{v}_r[n]$ are assumed to be uncorrelated. Secondly, the structure of $\mathbf{R}_{ss}^{(0)}$ depends on the specific noise model under consideration [21]. Specifically, it is given by

1) $\mathbf{R}_{ss}^{(0)} = \mathbf{I}_{NP} \otimes \mathbf{D}_L$, where $\mathbf{D}_L \in \mathbb{D}_L$ and $\mathbb{D}_L$ denotes the set of diagonal covariance matrices of dimension L,
2) $\mathbf{R}_{ss}^{(0)} = \mathbf{I}_{NP} \otimes \mathbf{A}_L$, where $\mathbf{A}_L \in \mathbb{A}_L$ and $\mathbb{A}_L$ denotes the set of positive semidefinite matrices of dimension L,
3) $\mathbf{R}_{ss}^{(0)}$ is block-Toeplitz with block size L and each block is diagonal.

Now we stack $\mathbf{y}_s$ and $\mathbf{y}_r$ into one long vector

$$\mathbf{y} = \left[\mathbf{y}_s^T, \mathbf{y}_r^T\right]^T. \tag{3}$$

Assuming $\mathbf{y}$ to be zero-mean proper complex Gaussian we can reformulate (1) as

$$\begin{aligned} \mathcal{H}_0 &: \mathbf{y} \sim \mathcal{CN}_{2LNP}(\mathbf{0}, \mathbf{R}_0), \\ \mathcal{H}_1 &: \mathbf{y} \sim \mathcal{CN}_{2LNP}(\mathbf{0}, \mathbf{R}_1), \end{aligned} \tag{4}$$

with

$$\mathbf{R}_0 = \mathrm{E}\left[\mathbf{y}\mathbf{y}^H | \mathcal{H}_0\right] = \begin{bmatrix} \mathbf{R}_{ss}^{(0)} & \mathbf{0} \\ \mathbf{0} & \mathbf{R}_{rr} \end{bmatrix}, \tag{5}$$

and

$$\mathbf{R}_1 = \mathrm{E}\left[\mathbf{y}\mathbf{y}^H | \mathcal{H}_1\right] = \begin{bmatrix} \mathbf{R}_{ss}^{(1)} & \mathbf{R}_{sr} \\ \mathbf{R}_{rs} & \mathbf{R}_{rr} \end{bmatrix}. \tag{6}$$

In order to derive the GLRT it would be necessary to obtain the maximum likelihood estimates (MLE) of $\mathbf{R}_0$ and $\mathbf{R}_1$. However, this would involve finding the MLE of a block-Toeplitz matrix for which there exists no closed-form solutions [22]. For this reason we make use of the approximation proposed in [18], where it is shown that the log-likelihood parameterized by a block-Toeplitz covariance matrix converge asymptotically ($N \to \infty$) to the log-likelihood parameterized by a block-circulant covariance matrix. Moreover, we exploit that a block-circulant covariance matrix can be block-diagonalized by the DFT matrix and a block-diagonal covariance matrix in turn has a closed-form MLE.

III. Derivation of the GLRT

In order to derive a closed-form expression for the (asymptotic) GLRT, we follow the approach in [18] and transform the samples from both arrays into the frequency domain as follows

$$\mathbf{z}_\clubsuit = (\mathbf{L}_{NP,N} \otimes \mathbf{I}_L)(\mathbf{F}_{NP} \otimes \mathbf{I}_L)^H \mathbf{y}_\clubsuit \in \mathbb{C}^{LNP}, \tag{7}$$

where $\otimes$ denotes the Kronecker product, $\mathbf{L}_{NP,N}$ is the commutation matrix,[2] and $\mathbf{F}_{NP}$ is the DFT matrix of size NP. Similar to the time domain we stack $\mathbf{z}_s$ and $\mathbf{z}_r$ into a vector

$$\mathbf{z} = [\mathbf{z}_s^T, \mathbf{z}_r^T]^T, \tag{8}$$

to reformulate the hypotheses (4) as

$$\begin{aligned} \mathcal{H}_0 &: \mathbf{z} \sim \mathcal{CN}_{2LNP}(\mathbf{0}, \mathbf{S}_0), \\ \mathcal{H}_1 &: \mathbf{z} \sim \mathcal{CN}_{2LNP}(\mathbf{0}, \mathbf{S}_1). \end{aligned} \tag{9}$$

Given $M \geq LP$ independent and identically distributed (i.i.d.) realizations of $\mathbf{z}$, the GLR is given by the ratio of

[1] Note that the superscripts (0) and (1) emphasize that it is the covariance matrix obtained under the null hypothesis or the alternative, respectively.

[2] The commutation matrix fulfills the following equation: $\mathrm{vec}(\mathbf{A}) = \mathbf{L}_{MN,N} \, \mathrm{vec}\left(\mathbf{A}^T\right)$ for an $M \times N$ matrix $\mathbf{A}$.

the determinants of the MLEs of the covariance matrices [14]

$$\Lambda^{\frac{1}{M}} = \frac{p(\mathbf{z}_0, \cdots, \mathbf{z}_{M-1}; \hat{\mathbf{S}}_0)}{p(\mathbf{z}_0, \cdots, \mathbf{z}_{M-1}; \hat{\mathbf{S}}_1)} = \frac{\det\left(\hat{\mathbf{S}}_1\right)}{\det\left(\hat{\mathbf{S}}_0\right)}, \qquad (10)$$

where $\hat{\mathbf{S}}_0$ and $\hat{\mathbf{S}}_1$ denote the MLEs of $\mathbf{S}_0$ and $\mathbf{S}_1$, respectively.

Similarly to the time-domain covariance matrices $\mathbf{R}_0$ and $\mathbf{R}_1$, we partition the frequency-domain covariance matrices into blocks as follows

$$\mathbf{S}_0 = \begin{bmatrix} \mathbf{S}_{ss}^{(1)} & \mathbf{0} \\ \mathbf{0} & \mathbf{S}_{rr} \end{bmatrix}, \qquad (11)$$

and

$$\mathbf{S}_1 = \begin{bmatrix} \mathbf{S}_{ss}^{(1)} & \mathbf{S}_{sr} \\ \mathbf{S}_{rs} & \mathbf{S}_{rr} \end{bmatrix}, \qquad (12)$$

where each block is given by the (cross) covariance matrix of $\mathbf{z}_s$ and $\mathbf{z}_r$, respectively. The permutation and transformation in (7) is designed such that the corresponding (cross) covariance matrices all have a block-diagonal structure. Specifically, $\mathbf{S}_{ss}^{(1)}$, $\mathbf{S}_{sr}$, and $\mathbf{S}_{rr}$ are block-diagonal with block size LP, and depending on the noise model $\mathbf{S}_{ss}^{(0)}$ is given by [21]

1) $\mathbf{S}_{ss}^{(0)} = \mathbf{I}_{NP} \otimes \tilde{\mathbf{D}}_L$, where $\tilde{\mathbf{D}}_L \in \mathbb{D}_L$,
2) $\mathbf{S}_{ss}^{(0)} = \mathbf{I}_{NP} \otimes \tilde{\mathbf{A}}_L$, where $\tilde{\mathbf{A}}_L \in \mathbb{A}_L$,
3) $\mathbf{S}_{ss}^{(0)}$ is diagonal.

A. MLEs of $\mathbf{S}_0$ and $\mathbf{S}_1$

Given the sample covariance matrix of M i.i.d. samples of $\mathbf{z}$,

$$\mathbf{Q} = \frac{1}{M}\sum_{m=0}^{M-1} \mathbf{z}_m \mathbf{z}_m^H = \begin{bmatrix} \mathbf{Q}_{ss} & \mathbf{Q}_{sr} \\ \mathbf{Q}_{rs} & \mathbf{Q}_{rr} \end{bmatrix}, \qquad (13)$$

the MLE of $\mathbf{S}_0$ may be easily obtained by considering its block-diagonal structure, i.e.

$$\hat{\mathbf{S}}_0 = \begin{bmatrix} \hat{\mathbf{S}}_{ss}^{(0)} & \mathbf{0} \\ \mathbf{0} & \mathrm{diag}_{LP}\left(\mathbf{Q}_{rr}\right) \end{bmatrix}, \qquad (14)$$

where the noise structure-dependent MLEs, $\hat{\mathbf{S}}_{ss}^{(0)}$, were derived in [21] and are given by

1) $\hat{\mathbf{S}}_{ss}^{(0)} = \mathbf{I}_{NP} \otimes \left(\frac{1}{NP}\sum_{i=1}^{NP} \mathrm{diag}\left([\mathbf{Q}_{ss}]_i\right)\right)$,
2) $\hat{\mathbf{S}}_{ss}^{(0)} = \mathbf{I}_{NP} \otimes \left(\frac{1}{NP}\sum_{i=1}^{NP} [\mathbf{Q}_{ss}]_i\right)$,
3) $\hat{\mathbf{S}}_{ss}^{(0)} = \mathrm{diag}\left(\mathbf{Q}_{ss}\right)$,

where $[\mathbf{Q}_{ss}]_i$ denotes the ith block of dimension L on the main diagonal of $\mathbf{Q}_{ss}$. The structure of $\mathbf{S}_1$ is given by a 2×2 block matrix, where each block itself is a block-diagonal matrix. Deriving the MLE of this matrix may seem to be more involved. However, it can be observed that it is always possible to permute the blocks in $\mathbf{S}_1$ such that another block-diagonal matrix with block size $2LP$ can be obtained. The MLE of this permuted matrix is again given by the block-diagonal matrix obtained from the corresponding blocks of the sample covariance matrix [17]. After applying the inverse permutation to the MLE, we end up with

$$\hat{\mathbf{S}}_1 = \begin{bmatrix} \mathrm{diag}_{LP}\left(\mathbf{Q}_{ss}\right) & \mathrm{diag}_{LP}\left(\mathbf{Q}_{sr}\right) \\ \mathrm{diag}_{LP}\left(\mathbf{Q}_{rs}\right) & \mathrm{diag}_{LP}\left(\mathbf{Q}_{rr}\right) \end{bmatrix}. \qquad (15)$$

B. GLRT

Finally, we can plug in (14) and (15) into (10) to obtain

$$\Lambda^{\frac{1}{M}} = \det\left(\mathbf{D}\right)\det\left(\mathbf{I} - \mathbf{C}\mathbf{C}^H\right), \qquad (16)$$

where $\mathbf{D} = \left(\hat{\mathbf{S}}_{ss}^{(0)}\right)^{-1/2}\mathrm{diag}_{LP}\left(\mathbf{Q}_{ss}\right)\left(\hat{\mathbf{S}}_{ss}^{(0)}\right)^{-1/2}$ and $\mathbf{C} = \mathrm{diag}_{LP}\left(\mathbf{Q}_{ss}\right)^{-1/2}\mathrm{diag}_{LP}\left(\mathbf{Q}_{sr}\right)\mathrm{diag}_{LP}\left(\mathbf{Q}_{rr}\right)^{-1/2}$, and where we exploited the properties of the determinant of block matrices. Note that only the first term in (16) depends on the noise structure through $\hat{\mathbf{S}}_{ss}^{(0)}$. Furthermore, we observe that $\mathbf{D}$ is a coherence matrix that only depends on the correlations between observations at the SC, whereas $\mathbf{C}$ is a cross-coherence matrix that depends on the cross-correlations between SC and RC. After noticing that both $\mathbf{D}$ and $\mathbf{C}$ are block-diagonal matrices with block size LP, we may further simplify (16) as follows

$$\Lambda^{\frac{1}{M}} = \prod_{k=1}^{N}\prod_{l=1}^{LP} \lambda_k^{(l)}\left[1 - \left(\kappa_k^{(l)}\right)^2\right], \qquad (17)$$

where $\lambda_k^{(l)}$ denotes the lth eigenvalue of the kth diagonal block of $\mathbf{D}$, which depends on the noise models 1)-3), and $\kappa_k^{(l)}$ denotes the lth eigenvalue of the kth block of $\mathbf{C}$. Finally, the GLRT is given by

$$\Lambda^{\frac{1}{M}} \underset{\mathcal{H}_1}{\overset{\mathcal{H}_0}{\gtrless}} \eta, \qquad (18)$$

where η is selected to guarantee a given probability of false alarm.

It should be noted that $\lambda_k^{(l)}$ and $\kappa_k^{(l)}$ can be given an interpretation. Recall the linear transformation (7) that transforms the samples into the frequency domain and orders them such that every LP consecutive samples are those frequency components that are separated by multiples of the cycle frequency $2\pi/P$ [18]. These frequencies may be correlated if the signal is CS, and they are uncorrelated for a WSS process. It can be observed that $\lambda_k^{(l)}$ are the sample canonical correlations between frequency components of the SC observations separated by multiples of $2\pi/P$. Moreover, considering the products over these $\lambda_k^{(l)}$ individually, this product is the GLRT for detecting the presence of CS at a single channel (here the SC) [18], [21]. Similarly, $\kappa_k^{(l)}$ are the sample canonical correlations between frequency components of SC and RC observations.

C. Threshold selection

In order to find the threshold for a given probability of false alarm p_{fa}, we exploit the invariances of the test statistic. Note that we can multiply $\mathbf{z}$ with any matrix of the structure of $\mathbf{S}_0$ without modifying the likelihood ratio, i.e., it is invariant to these transformations. Hence, without loss of generality, we can assume that the observations under the null hypothesis are whitened. Thus, to find the threshold for any arbitrary process, we can run numerical simulations with temporally and spatially white processes.

IV. Numerical results

We evaluate the performance of the GLRT for the different noise models using Monte Carlo simulations.[3] According to our model in (1), we generate the CS signal $\mathbf{s}[n]$ as a QPSK-signal with rectangular pulse shaping. The number of samples per symbol is equal to the cycle period P. Furthermore, the frequency-selective channels $\mathbf{H}_s[n]$ and $\mathbf{H}_r[n]$ are both Rayleigh-fading channels with a delay spread of 10 times the symbol duration and an exponential power delay profile. The SNR at the surveillance array is set to $\text{SNR}_s = -10$ dB and at the reference array it is set to $\text{SNR}_s = -5$ dB. In each Monte Carlo simulation we draw new realizations of the channels. We consider simulation setups with the noise structures in Model 1) and Model 3), i.e., temporally white or colored, and spatially uncorrelated noise. Here, the noise terms are independent between SC and RC, white Gaussian, or colored Gaussian generated with a moving average filter of order 10 and uncorrelated among antennas. Moreover, in the figures presented in this section, 1) refers to the detector exploiting noise structure from Model 1, 2) and 3) refer to the detectors that exploits only temporal or spatial structure of the noise, respectively.

In Figure 1 we compare the receiver operating characteristic (ROC) curves of the three proposed detectors 1) - 3), which exploit various degrees of noise structure. Detector 2) only considers temporal structure, Detector 3) only considers spatial structure, whereas Detector 1) takes into account both. Since the noise in our example is temporally and spatially white, Detector 1) outperforms Detectors 2) and 3), but taking into account temporal structure is more advantageous. Moreover, all detectors outperform competing approaches, namely, the GLRT from [17] that does not exploit the noise structure, the correlated subspace detector proposed in [14], and the cross-correlation detector [9].

Similar observations can be made in Figure 2, where we compare the ROCs of the various detectors for simulations under noise Model 3. As can be observed, Detector 3), which matches the model, performs best among the competing ones. Interestingly, applying the white noise detectors 1) and 2) decreases the performance substantially. The reason for this is that Detectors 1) and 2) underfit noise model 3), which has many more degrees of freedom

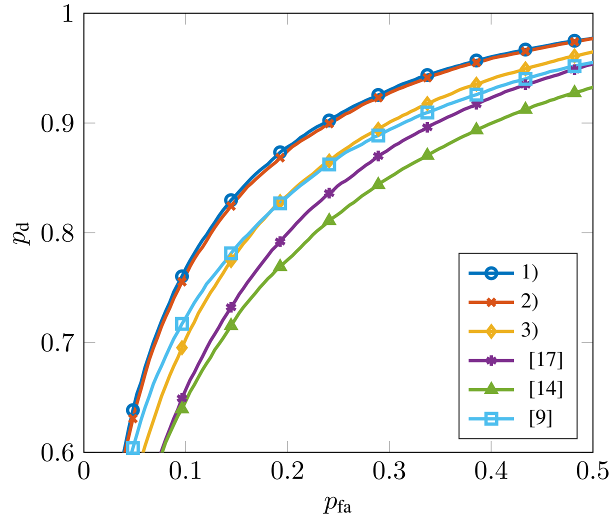

Fig. 1: ROC for a scenario with temporally white and spatially uncorrelated noise (Model 1) for $P = 2$, $N = 16$, $L = L_I = 4$, $M = 32$, $\text{SNR}_s = -10$ dB, and $\text{SNR}_r = -5$ dB.

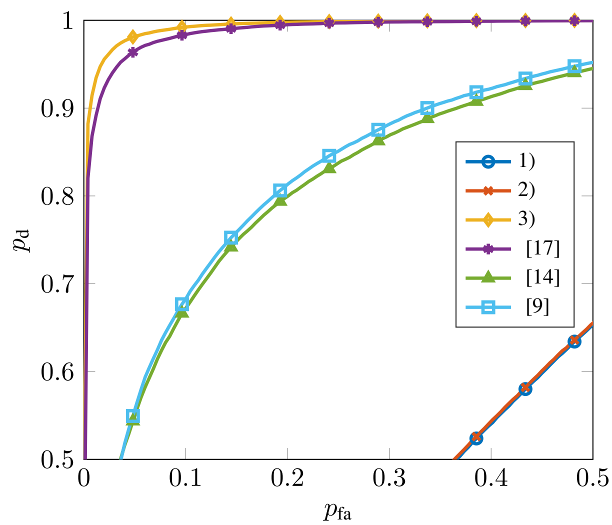

Fig. 2: ROC for a scenario with temporally colored and spatially uncorrelated noise (Model 3) for $P = 2$, $N = 16$, $L = L_I = 4$, $M = 32$, $\text{SNR}_s = -10$ dB, and $\text{SNR}_r = -5$ dB.

as captured by 1) and 2). Hence, in general accounting for the temporal structure is essential. Note that the influence of the spatial structure is not as large as the related degrees of freedom depend on L, whereas the number of free parameters of the model corresponding to the temporal structure depend on N, which is generally much larger.

Acknowledgment

S. Horstmann, P. J. Schreier, and A. Pries were supported by the German Research Foundation (DFG) under grant SCHR 1384/6-1. The work of D. Ramírez was supported by the Ministerio de Ciencia, Innovación y Universidades under grant TEC2017-92552-EXP (aMBI-

[3]Matlab code is available for download from: https://github.com/SSTGroup/Cyclostationary-Signal-Processing

TION), by the Ministerio de Ciencia, Innovación y Universidades, jointly with the European Commission (ERDF), under grant TEC2017-86921-C2-2-R (CAIMAN), by The Comunidad de Madrid under grant Y2018/TCS-4705 (PRACTICO-CM), and by the German Research Foundation (DFG) under grant RA 2662/2-1.

References

[1] H. D. Griffiths and C. J. Baker, "Passive coherent location radar systems. Part 1: Performance prediction," *IEE Proc. Radar Sonar Navig.*, vol. 152, pp. 153–159, June 2005.

[2] R. Tao, H. Wu, and T. Shan, "Direct-path suppression by spatial filtering in digital television terrestrial broadcasting-based passive radar," *IET Radar, Sonar, Navigation*, vol. 4, pp. 791–805, Sept. 2010.

[3] F. Colone, D. O'Hagan, P. Lombardo, and C. Baker, "A Multistage Processing Algorithm for Disturbance Removal and Target Detection in Passive Bistatic Radar," *IEEE Trans. on Aerospace, Electr. Syst.*, vol. 45, pp. 698–722, Apr. 2009.

[4] J. E. Palmer and S. J. Searle, "Evaluation of adaptive filter algorithms for clutter cancellation in passive bistatic radar," in *IEEE Radar Conference*, (Atlanta, GA, USA), pp. 493–498, 2012.

[5] R. Zemmari, U. Nickel, and W.-D. Wirth, "GSM passive radar for medium range surveillance," in *Proc. Eur. Radar Conf. (EuRAD)*, (Rome, Italy), pp. 49–52, 2009.

[6] D. O'Hagan, F. Colone, C. Baker, and H. Griffiths, "Passive bistatic radar (PBR) demonstrator," in *Proc. IET Int. Radar Syst. Conf.*, (Edinburgh, UK), pp. 1–5, 2007.

[7] F. Colone, R. Cardinali, P. Lombardo, O. Crognale, A. Cosmi, A. Lauri, and T. Bucciarelli, "Space-time constant modulus algorithm for multipath removal on the reference signal exploited by passive bistatic radar," *IET Radar, Sonar, Navigation*, vol. 3, no. 3, pp. 253–264, 2009.

[8] G. Smith, K. Chetty, C. Baker, and K. Woodbridge, "Extended time processing for passive bistatic radar," *IET Radar, Sonar, Navigation*, vol. 7, pp. 1012–1018, Dec. 2013.

[9] J. Liu, H. Li, and B. Himed, "On the performance of the cross-correlation detector for passive radar applications," *Signal Process.*, vol. 113, pp. 32–37, 2015.

[10] S. D. Howard and S. Sirianunpiboon, "Passive radar detection using multiple transmitters," in *Proc. 47th Asilomar Conf. Signals, Syst., Comput.*, (Pacific Grove, CA, USA), pp. 945–948, Nov. 2013.

[11] D. E. Hack, L. K. Patton, and B. Himed, "Detection in passive MIMO radar networks," *IEEE Trans. on Signal Process.*, vol. 62, pp. 780–785, June 2014.

[12] I. Santamaría, L. L. Scharf, D. Cochran, and J. Vía, "Passive detection of rank-one signals with a multiantenna reference channel," in *Proc. 24th European Signal Proc. Conf. (EUSIPCO)*, (Budapest, Hungary), pp. 140–144, 2016.

[13] H. Wang, Y. Wang, L. L. Scharf, and I. Santamaría, "Canonical correlations for target detection in a passive radar network," in *Proc. 50th Asilomar Conf. Signals, Syst., Comput.*, (Pacific Grove, CA, USA), pp. 1159 – 1163, 2016.

[14] I. Santamaría, L. L. Scharf, J. Vía, H. Wang, and Y. Wang, "Passive detection of correlated subspace signals in two MIMO channels," *IEEE Trans. on Signal Process.*, vol. 65, pp. 5266–5280, Oct. 2017.

[15] I. Santamaría, J. Vía, L. L. Scharf, and Y. Wang, "A GLRT approach for detecting correlated signals in white noise in two MIMO channels," in *Proc. 25th European Signal Proc. Conf. (EUSIPCO)*, (Kos, Greece), pp. 1395–1399, 2017.

[16] W. A. Gardner, W. A. Brown, and C. Chen, "Spectral correlation of modulated signals: Part II - digital modulation," *IEEE Trans. on Comms.*, vol. Com-35, pp. 595–601, June 1987.

[17] S. Horstmann, D. Ramírez, and P. J. Schreier, "Two-channel passive detection exploiting cyclostationarity," in *Proc. 27th European Signal Proc. Conf. (EUSIPCO)*, (A Coruña, Spain), 2019.

[18] D. Ramírez, P. J. Schreier, J. Vía, I. Santamaría, and L. L. Scharf, "Detection of multivariate cyclostationarity," *IEEE Trans. on Signal Process.*, vol. 63, pp. 5395–5408, Oct. 2015.

[19] A. Pries, D. Ramírez, and P. J. Schreier, "LMPIT-inspired tests for detecting a cyclostationary signal in noise with spatio-temporal structure," *IEEE Trans. on Wireless Comms.*, vol. 17, pp. 6321–6334, Sept. 2018.

[20] E. D. Gladyshev, "Periodically correlated random sequences," *Soviet Math. Dokl.*, vol. 2, pp. 385–388, 1961.

[21] A. Pries, D. Ramírez, and P. J. Schreier, "Detection of cyclostationarity in the presence of temporal or spatial structure with applications to cognitive radio," in *Proc. IEEE Int. Conf. Acoust., Speech, Signal Proc. (ICASSP)*, (Shanghai, China), pp. 4249–4253, 2016.

[22] J. P. Burg and D. G. Luenberger, "Robust estimation of structured covariance matrices," *IEEE Trans. on Signal Process.*, vol. 70, pp. 963–974, Sept. 1982.